International Journal of Advances in Engineering and Management (IJAEM)
Volume 3, Issue 7 July 2021, pp: 881-895 www.ijaem.net ISSN: 2395-5252

# Microgrid Based Wind-Solar Cogeneration Using Bi-Directional Voltage Source Converters

[1]J.Narmatha, [2] Dr.S.Anbumalar
*PG Student, Head of the Department, Department of Power Electronics and Drivess*
*Sri Manakula Vinayagar Engineering College, Puducherry, India*

Submitted: 25-06-2021 Revised: 04-07-2021 Accepted: 07-07-2021

**ABSTRACT**
The renewable energy sources like sun and wind are the alternate sources of green power generation which can ease the power demand problems. This paper presents the control approach for power flow management of a gridconnected hybrid photovoltaic (PV)–wind-battery-based system with bidirectional dc–dc converter. The main objective of this project is to minimize the converters.The proposed framework is to satisfy the heap need, manage the force stream from different sources, infuse the extra force into the network, and charge the battery from the matrix at whatever point fundamental. This can improves the unwavering quality and proficiency of the framework. The proposed Hybrid framework with the MPPT controlled Bidirectional DC-DC converters and Voltage managed Inverter for independent application is created and recreated in MATLAB climate. The main objective is combined application of renewable energy concepts and control systems for the qualitative and quantitative improvement of electricity generated from solar and wind sources. The power generated from the general solar and wind sources is generally at a certain level. But the addition of solar and wind sources and control systems will surely be more in quantity and by the application of power electronic converters the power generated will be more efficient.

**Keywords—** Solar Photovoltaic (PV), Wind Energy, Hybrid Energy System, Bidirectional DC-DC Converter, Maximum Power-Point Tracking, Matlab Software.

## I. Introduction:

In the current pattern, Renewable fuel sources are appealing decisions for giving force in where a relationship to the utility organization is either unrealistic or unduly expensive. As electric conveyance innovation ventures into one century from now, a few patterns have become recognizable which will alter the necessities of energy conveyance. The always expanding energy utilization, taking off esteem and expendable nature of petroleum products, and furthermore the demolishing global climate have made improved interest in green force age frameworks. Inexhaustible sources have acquired overall consideration due to fast exhaustion of petroleum derivatives related to developing energy request [1].

The energy that is gathered from sustainable assets is called environmentally friendly power, which are normally renewed on a human timescale, like daylight, wind, downpour, tides, waves, and geothermal warmth [2]. Sustainable power gives energy in four regions like: power age, air and water warming/cooling, transportation, and provincial (off-network) energy administrations [3].

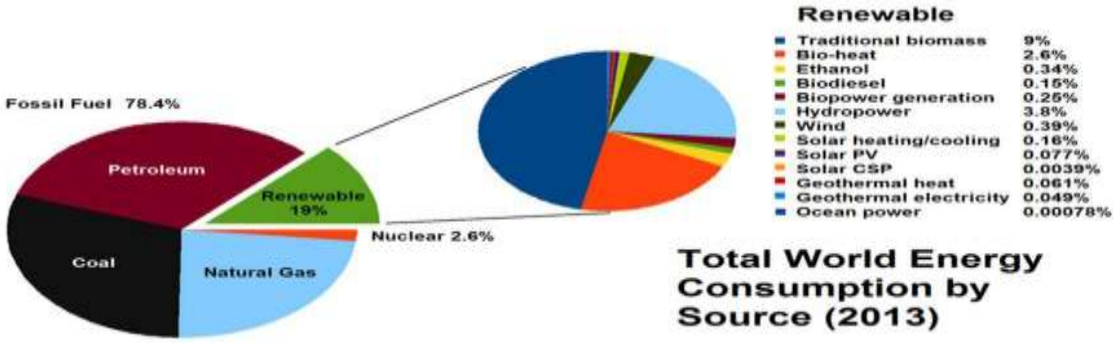


Fig. 1. World energy consumption by renewable sources accounted for 19% in 2012

International Journal of Advances in Engineering and Management (IJAEM)
Volume 3, Issue 7 July 2021, pp: 881-895 www.ijaem.net ISSN: 2395-5252

In light of REN21's report (2016), inexhaustible sources contributed 19.2% to people's global energy utilization and 23.7% to their age of power in 2014 and 2015, yearly. This energy utilization is parted as 8.9% getting back from old biomass, 4.2% as energy (present day biomass, energy and sunlight based warmth), 3.9% hydroelectricity and 2.2% is power from wind, sun oriented, geothermal, and biomass.[4-8] Worldwide interests in inexhaustible advances added up to very US$286 billion of every 2015, by nations like China and furthermore U.S. in wind, hydro, sun powered and bio-powers. Worldwide, there are 7.7 million positions identified with the environmentally friendly power businesses, with sun oriented photovoltaic being the main sustainable manager. Starting at 2015, very 50% of all new power ability around the world introduced was inexhaustible [9-10].

Reasonable force source springs from regular systems that are re-energized never endingly. In its contrasted shapes, it gets straightforwardly from the sun, or from warmth delivered significant among the planet. Encased inside the definition is force and warmth made from daylight, wind, ocean, hydro power, biomass based energy resources, and bio-forces and substance segment got from practical resources. Maintainable force source resources are pivotal open entryways. For energy intensity existing over wide land territories, in qualification to energy source options that are engaged in an exceptionally limited scope of states [11].

Before the period of coal during nineteenth century, practically all energy utilized was sustainably created. Not a marvel, the most seasoned popular utilization of sustainable power inside the old style was biomass to fuel fires, dates from 790,000 years past [12-14]. Utilization of biomass for chimney neglected to get ordinary till a few a long time later, some time or another somewhere in the range of 200,000 and 400,000 years past [15]. Doubtlessly the second most seasoned use of environmentally friendly power is tackling the breeze to drive ships over water. This perception might be gotten back from 7000 years, to ships on the stream [16] in the hour of written history. The main wellsprings of old sustainable power were human work, creature power, water power, grain smashing windmills, traditional biomass. A diagram of energy use inside the US until 1900 shows oil and petroleum product had indistinguishable significance in 1900 as wind and sun oriented had in 2010[17-20].

## SOLAR WIND COGERATION USING MICROGRID

### SYSTEM DESCRIPTION OF SOLAR POWER

The photovoltaic (PV) generation systems are expected to increase significantly worldwide. PVs are an attractive source of renewable energy for distributed urban power generation due to their relatively small size and noiseless operation. PV generating technologies have the advantage that more units can be added to meet load increase demand. The basic block diagram of grid connected PV power generation system is shown in Fig. The PV power generation system consists of following major blocks:

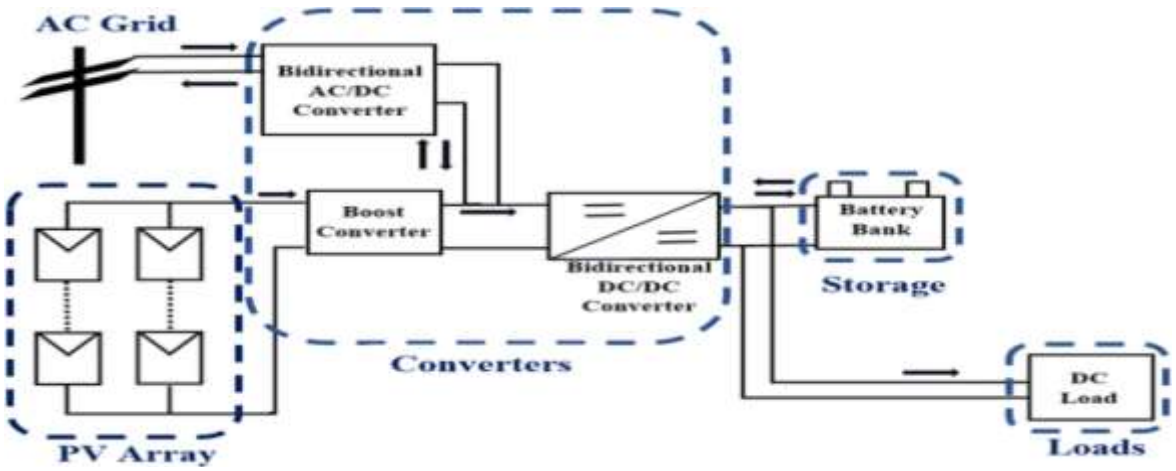

International Journal of Advances in Engineering and Management (IJAEM)
Volume 3, Issue 7 July 2021, pp: 881-895 www.ijaem.net ISSN: 2395-5252

**PV Array:** A PV unit consists of number of PV cells that converts the energy of light directlyinto electricity (DC) using photovoltaic effect.

**Bidirectionalconverter**:Bidirectional DC-DC converters are used in applications where bidirectional power flow may be required. A commonplace framework comprises of a full-connect power stage on the high-voltage (HV) side, which is secluded from a full-connect or a current-took care of push-pull stage on the low-voltage (LV) side.

**Boost converter:**A lift converter is a DC-to-DC power converter that means up voltage from its contribution to its yield. It is a class of exchanged mode power supply containing in any event two semiconductors and at any rate one energy stockpiling component: a capacitor, inductor, or the two in mix.

**Battery:**A battery is a force source comprising of at least one electrochemical cells with outer associations for fueling electrical gadgets like spotlights, cell phones, and electric vehicles. At the point when a battery is providing electric force, its positive terminal is the cathode and its adverse terminal is the anode.

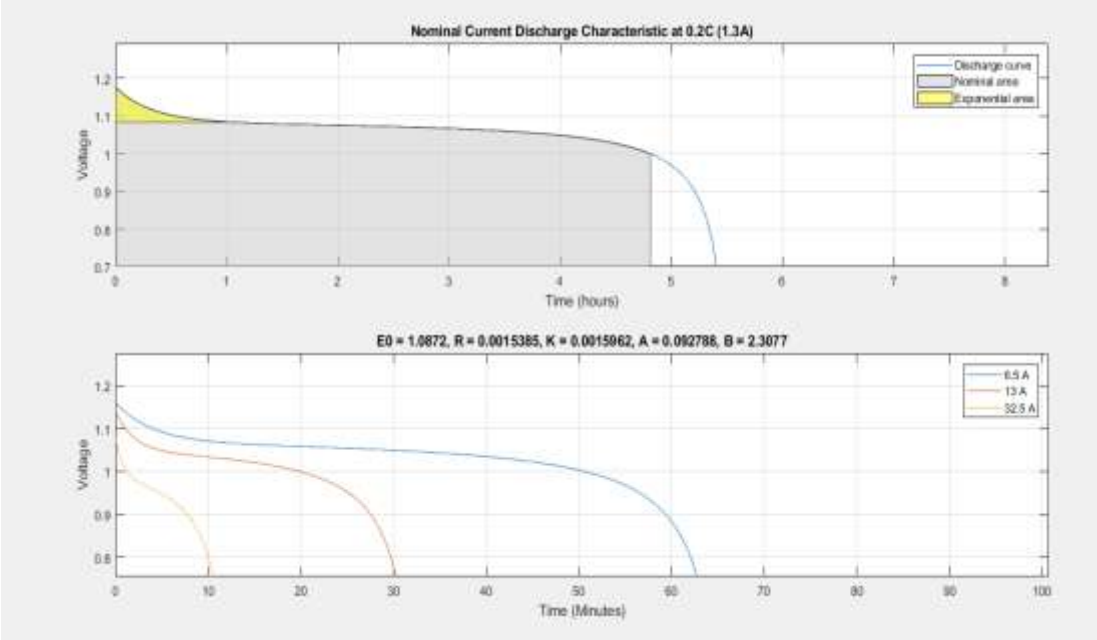


**Inverter:** Inverter is used to convert DC output of PV unit to AC power.

**Grid:** The output power of inverter is given to the nearby electrical grid for thepower generation.

**MPPT:** In order to utilize the maximum power produced by the PV modules, thepower conversion equipment has to be equipped with a maximum power point tracker (MPPT). It is a device which tracks the voltage at where the maximum power is utilized at all times.

**Sub system model and Expression:**

In this paper, a PV array is highly-nonlinear but reflects no dynamic performance on the transient stability of the system. The model of the PV generator is given in Appendix A whereas the dc cable dynamics in Fig. 1 are modeled as following:

$$V_{pv} = V_{dc} + R_{dc} I_{pv} + L_{dc} \frac{di_{pv}}{dt} \quad (1)$$

The $I_{pv}$-$V_{pv}$ characteristics of the PV array are shown in Fig. 2. At any solar irradiance level, there is an optimal operating point ($I_{pv}^{o} - V_{pv}^{o}$) corresponding to the maximum generated PV power. As shown in Fig. 1, the MPPT algorithm of the PV array (MPPT,) uses the solar irradiance level (S) to determine the optimal value of the dc link voltage that corresponds to the generation of the maximum PV Power.

The nominal voltage of the PV arrays is designed at 1457V. With nowadays improvements in the centralized power converters, PV arrays can be directly connected to a dc-link with nominal de voltage up to 1500V at 2.0 MVA.

International Journal of Advances in Engineering and Management (IJAEM)
Volume 3, Issue 7 July 2021, pp: 881-895 www.ijaem.net ISSN: 2395-5252

**GRID SIDE VOLTAGE SOURCE INVERTER:**

Grid-Side Voltage Source Inverter is the ac-side of the VSI is terminated by an inductive filter ($L_f$) with an internal resistance ($R_f$) and a shunt capacitor ($C_f$). The root-mean-square (rms) value of the three phase terminalsi$_c$, respectively. The utility-grid-impedance comprises currents, respectively. The Utility grid impedance comprises an inductive part in series with the equivalent resistance of the line ($R_g$);$V_g$and $I_g$are the utility grid three phase rms voltage and current respectively.

The $L_f$ and $C_f$ filter and the utility grid impedance are called as modelled as fallowing;

$$V_c = V_f + R_f I_c + L_f \frac{di_c}{dt} + jwL_f L_c \quad (2)$$

$$V_f = V_g + R_g I_g + L_g \frac{di_g}{dt} + jwL_g L_g \quad (3)$$

$$I_c = L_g + C_f \frac{dv_f}{dt} + jwC_f V_f \quad (4)$$

To avoid the over-modulation of the VSI, the design of the PV array should consider the coordination between the MPPT voltage of the PV array, i.e., Vdc, and the rms voltage at the point-of-common coupling (PCC), i.e., $V_f$ under all irradiance levels. In power converters, the pulse-width-modulation (PWM) and the switching pattern is dictated by the ratio between the ac and the de voltage such that $V_c = mV_{ac}/2$, where m is the modulation signal in complex vectors.

The VSI is regulated by the vector control scheme where a phase-locked-loop (PLL) is used to synchronize the converter with the utility-grid . In (10), a PI controller ($G_\delta(S) = K_{p\delta}(S) + K_{i\delta}/S$)is implemented in the PLL structure to set the q -component of the PCC voltage ($V_{cq}$) to zero and generate the Synchronization angle δ(t), where $\delta(t) = \int w(t)dt$ . Under transient conditions, the angle δ(t) oscillates to resynchronize the converter with the Utility grid and eventually becomes zero in the steady state conditions.

$$w = W^\circ + \frac{V^c f_q}{V^\circ f_d} \qquad K_\delta(s) \quad (5)$$

As shown in (6), the main advantage of the vector control is the decoupling between the active and reactive power regulation, As $V_{cq}$ is set to zero by (5) and assuming $V_{cd}$ is constant, the active power injection from the VSI ($P_{vsi}$) can be regulated by controlling $I_{cd}$ whereas the reactive power ($Q_{vsi}$) solely dependent on $I_{cq}$

$$P_{vsi} = \text{Real}\{1.5V_c I_c^{-\text{Conjugate}}\} = 1.5\, V_{cd} I_{cd} \quad (6)$$

$$Q_{vsi} = \text{Imaginary}\{1.5V_c I_c^{-\text{Conjugate}}\} = -1.5\, V_{cd} I_{cq} \quad (7)$$

**3.4.2 DC-LINK VOLTAGE CONTROL:**

The dc-link voltage of the Back to Back VSCs ($V_{dc}$) is regulated to the optimal value ($V_{dc}$) (generated by MPPT ) as shown in (12). where a PI dc voltage controller ($K_{dc}(s) = k_{pdc} + k_{idc}/s$) is implemented

$$I_{cd}^* = -(V_{dc}^{*2} - V_{dc}^2) K_{dc}(s) \left(\frac{1}{1.5V_{fd}^\circ}\right) \quad (8)$$

Referring to Fig. 1, and as shown in (13), the rate of change of the energy in Cac is governed by the balance between the delivered wind and PV power ($P_{wind} + P_{pv}$) and the injected active power to the utility-grid (Pvsi), assuming a lossless converter.

$$\frac{1}{2} c_{dc} \frac{d}{dt} V_{dc}^2 = P_{wind} + P_{pv} - P_{vsi} \quad (9)$$

Where

$P_{wind} = Real\{1.5V_s I_s^{-conjugate}\}$ $and$ $P_{wind} = P_{pv} - P_{vsi}$ .

By regulating $V_{dc}$ in (9) the input, i.e. $P_{wind} + P_{pv}$ , and the output $P_{vsi}$,active powers are balanced in eq(9) and so the active power component is generated from (8).

By Regulating $V_{dc}$ in (8) the input i.e.,$P_{wind}$+$P_{pv}$ and the output $P_{vsi}$ ,active powers are balanced in (9),and so the active power component ($I^*_{cd}$) is generated from (8) .

Using (6)-(9) the open loop transfer function of the dc link voltagecontroller becomes ;$I_{vdc}(s) = \left(2k_{pdc} \Big/ \tau_k C_{dc}\right)\left((S + \frac{k_{idc}}{k_{pdc}}) / (S + \frac{1}{\tau_k})\right)\frac{1}{S^2}$

,Where $\frac{1}{\tau_k}$ is the bandwidth of the inner current controller of the VSI.Note that the $l_{vdc}(s)$has three poles;two at zero and one at $-\frac{1}{\tau_k}$.At Low frequencies ,the phasor angle of $l_{vdc}(j\omega) \approx -180°$ due to the double poles at zero.Therefore the controller parameters are selected such that $\frac{k_{idc}}{k_{pdc}} < \frac{1}{\tau_k}$.As the result,the phase angle of $l_{vdc}(j\omega)$ increases to a maximum value $\delta_m^{vdc} = sin^{-1}((1 - \tau_k \frac{k_{idc}}{k_{pdc}})/(1 + \tau_k \frac{k_{idc}}{k_{pdc}}))$ at a certain frequency ($\omega_c^{vdc}$) is selected as $\omega_m^{vdc}$which holds by choosing $k_{pdc} = C_{dc}\omega_c^{vdc}$ such that $|l_{vdc}(j\omega_c^{vdc})| = |l_{vdc}(j\omega_m^{vdc})| = 1$ and hence $\delta_m^{vdc}$ becomes the phase margin .By solving the proceeding equations the parameters of the dc link voltage controller can be determined.

**UTILITY GRID VOLTAGE:**

A PI ac voltage controller ($K_{ac}(s) = K_{pac} + K_{iac}/_S$)is used to regulate the PCC voltage $\bar{V}_f$by generating$I^*_{cq}$ that corresponds to the required

International Journal of Advances in Engineering and Management (IJAEM)
Volume 3, Issue 7 July 2021, pp: 881-895 www.ijaem.net ISSN: 2395-5252

reactive power to maintain a unity PCC voltage. The parameters turning of $K_{ac}(s)$ is similar to design of the dc voltage controller.

$$I_{cq}^{*} = -\left(V_{fd}^{*} - V_{fd}^{c}\right)K_{ac}(s)$$

As shown in fig.1 and (11), the injected currents to the utility grid are controlled using a PI ac current controller($K_i(s) = K_{pi} + {}^{K_{ii}}/_{s}$ ).

$$\bar{v}_c^c = (\bar{i}_c - \bar{i}_c^c)K_i(s) + j\omega^{\circ} L_f \bar{i}_c^c + \bar{v}_f^c \quad (11)$$

Where $j\omega^{\circ} L_f \bar{i}_c^c$and $\bar{v}_f^c$ are the decoupling and the feedforward loop, respectively.The current controller $K_{i\,(s)}$ is designed fallowing the approach described for $G_{i\,(s)}$.

It should be noted that the measured ac quantities, i.e., $i_c$ and $v_f$, are transformed to the converter reference frame whereas the controller output signals, i.e.,$v_c$,should be retransformed to the grid reference frame to accurately model the influence of the PLL on the system dynamics. The frame transformation is mathematically represented in (12), assuming the angle difference between the two frames is very small such that $\cos\delta \approx 1$ and $\sin\delta \approx 0$.

$$\begin{aligned} \bar{i}_c^c &= (1 - j\delta)\bar{i}_c, \\ \bar{v}_f^c &= (1 - j\delta)\bar{v}_f, \\ \bar{v}_c &= (1 + j\delta)\bar{v}_c^c \ . \end{aligned} \quad (12)$$

Where the superscript "c" denotes the converter reference – frame.

**ABC –DQ TRANSFORMATION:**

The abc to $dq_0$ block utilizes a Park change to change a three-stage (abc) sign to a $dq_0$pivoting reference outline.The precise situation of the turning outline is given by the info $\omega t$, in rad.

The $dq_0$ to abc block uses utilizes an opposite Park change to change a $dq_0$turning reference edge to a three-stage (abc) signal. The angular situation of the pivoting outline is given by the information $\omega t$, in rad.

At the point when the pivoting outline arrangement at $\omega t$=0 is 90 degrees behind the phase A axis, a positive-succession signal with Mag=1 and Phase=0 degrees yields the accompanying dq values: d=1, q=0.

The Expression can be written as

$$V_d = \frac{2}{3}(V_a\, sin(\omega t) + V_b(sin(\omega t - 2\pi/3) + V_c\, sin(\omega t + 2\pi/3)) \quad (13)$$

$$V_q = \frac{2}{3}(V_a\, cos(\omega t) + V_b(cos(\omega t - 2\pi/3) + V_c\, cos(\omega t + 2\pi/3)) \quad (14)$$

$$V_0 = \frac{1}{3}(V_a + V_b + V_c) \quad (15)$$

$$V_a = V_d sin(\omega t) + V_q cos(\omega t) + V_0 \quad (16)$$

$$V_b = V_d sin(\omega t - 2\pi/3) + V_q cos(\omega t - 2\pi/3) + V_0 \quad (17)$$

$$V_c = V_d sin(\omega t + 2\pi/3) + V_q cos(\omega t + 2\pi/3) + V_0 \quad (18)$$

Phasor diagram for dq axis is drawn below.

International Journal of Advances in Engineering and Management (IJAEM)
Volume 3, Issue 7 July 2021, pp: 881-895 www.ijaem.net ISSN: 2395-5252

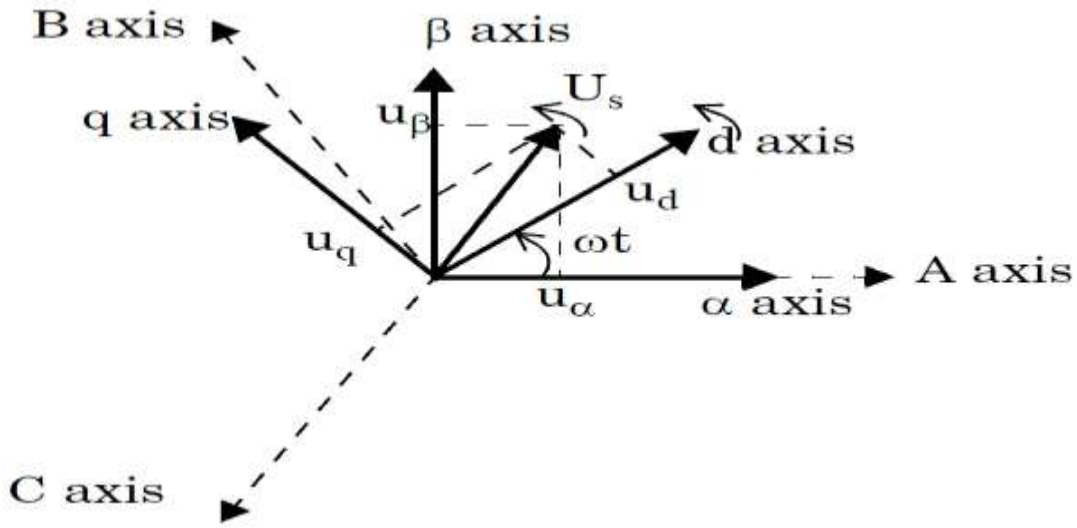


The block supports the two conventions used for the Park transformation:

- When the turning outline is lined up with phase A axis at t = 0, that is, at t = 0, the d-axis is aligned with the a-axis. This kind of Park change is otherwise known as the cosine-based Park transformation.
- When the turning outline is adjusted 90 degrees behind the phase A axis, that is, at t = 0, the q-axis is aligned with the a-axis. This kind of Park change is otherwise called the sine-based Park change. Utilize this change in Simscape Electrical Specialized Power Systems models with three-stage coordinated and offbeat machines.

The abc-to-dq0 transformation depends on the dq frame alignment at t = 0. The situation of the turning outline is given by ωt, where ω addresses the dq outline revolution speed.

When the rotating frame is aligned with the phase A axis, the following relations are obtained:

$$U_s = (u_d + j.u_q) = (u_a + j.u_\beta).e^{-j\omega t} = \frac{2}{3}.(u_a + u_b.e^{\frac{-j2\pi}{3}} + u_c.e^{\frac{j2\pi}{3}}).e^{-jwt} \quad (19)$$

$$u_0 = \frac{1}{3}(u_a + u_b + u_c) \quad (20)$$

$$\begin{bmatrix} u_d \\ u_q \\ u_0 \end{bmatrix} = \frac{2}{3} + \begin{bmatrix} cos(\omega t) & cos(\omega t - \frac{2\pi}{3}) & cos(\omega t + \frac{2\pi}{3}) \\ -sin(\omega t) & -sin(\omega t - \frac{2\pi}{3}) & -sin(\omega t + \frac{2\pi}{3}) \\ \frac{1}{2} & \frac{1}{2} & \frac{1}{2} \end{bmatrix} . \begin{bmatrix} u_a \\ u_b \\ u_c \end{bmatrix} \quad (21)$$

The inverse transformation is given by:

$$\begin{bmatrix} u_a \\ u_b \\ u_c \end{bmatrix} = \begin{bmatrix} cos(\omega t) & -sin(\omega t) & 1 \\ cos(\omega t - \frac{2\pi}{3}) & -sin(\omega t - \frac{2\pi}{3}) & 1 \\ cos(\omega t + \frac{2\pi}{3}) & -sin(\omega t + \frac{2\pi}{3}) & 1 \end{bmatrix} . \begin{bmatrix} u_d \\ u_q \\ u_0 \end{bmatrix} \quad (22)$$

When the rotating frame is aligned 90 degrees behind the phase A axis, the following relations are obtained:

$$U_s = (u_d + j.u_q) = (u_a + j.u_\beta).e^{-j(\omega t - \frac{\pi}{2})} \quad (23)$$

$$\begin{bmatrix} u_d \\ u_q \\ u_0 \end{bmatrix} = \frac{2}{3} + \begin{bmatrix} sin(\omega t) & sin(\omega t - \frac{2\pi}{3}) & sin(\omega t + \frac{2\pi}{3}) \\ cos(\omega t) & cos(\omega t - \frac{2\pi}{3}) & cos(\omega t + \frac{2\pi}{3}) \\ \frac{1}{2} & \frac{1}{2} & \frac{1}{2} \end{bmatrix} . \begin{bmatrix} u_a \\ u_b \\ u_c \end{bmatrix} \quad (24)$$

International Journal of Advances in Engineering and Management (IJAEM)
Volume 3, Issue 7 July 2021, pp: 881-895 www.ijaem.net ISSN: 2395-5252

The inverse transformation is given by:

$$\begin{bmatrix} u_a \\ u_b \\ u_c \end{bmatrix} = \begin{bmatrix} \sin(\omega t) & \cos(\omega t) & 1 \\ \sin(\omega t - \frac{2\pi}{3}) & \cos(\omega t - \frac{2\pi}{3}) & 1 \\ \sin(\omega t + \frac{2\pi}{3}) & \cos(\omega t + \frac{2\pi}{3}) & 1 \end{bmatrix} . \begin{bmatrix} u_d \\ u_q \\ u_0 \end{bmatrix} \quad (25)$$

**MPPT Algorithm:**

Incremental Conductance (IC) method overcomes the disadvantage of the perturb and observe method in tracking the peak power under fast varying atmospheric condition. This technique can decide if the MPPT has arrived at the MPP and furthermore quits irritating the working point. In the event that this condition isn't met, the course in which the MPPT working point should be irritated can be determined utilizing the connection between dl/dv and – I/V. This relationship is gotten from the way that dP/dV is negative when the MPPT is to one side of the MPP and positive when it is to one side of the MPP.The steady conductance calculation depends on the way that the slant of the bend power versus voltage (current) of the PV module is zero at the MPP, positive (negative) on its left and negative (positive) on the right. It can be written as

$$\frac{\Delta V}{\Delta P} = 0 \left(\frac{\Delta I}{\Delta P} = 0\right) at\ the\ MPP$$
$$\frac{\Delta V}{\Delta P} > 0 \left(\frac{\Delta I}{\Delta P} < 0\right) on\ the\ left$$
$$\frac{\Delta V}{\Delta P} < 0 \left(\frac{\Delta I}{\Delta P} > 0\right) on\ the\ right \quad (26)$$

By looking at the augmentation of the force versus the addition of the voltage (current) between two consecutives tests, the adjustment of the MPP voltage can be resolved.

**SYSTEM DESCRIPTION OF WIND ENERDY:**

In this configuration, wind generations are based on constant speed topologies with pitch control turbine.The generator is utilized in the proposed plot in view of its effortlessness, it doesn't need a different field circuit, it can acknowledge consistent and variable loads, and has characteristic insurance against impede.

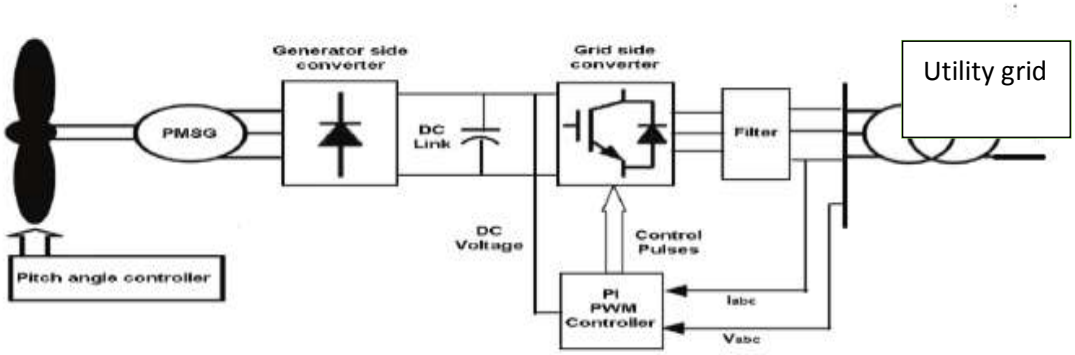


**Pulse width modulation:**

Pulse width modulation (PWM) is a regulation procedure that produces variable-width heartbeats to address the abundancy of a simple information signal. The yield exchanging semiconductor is on a greater amount of the ideal opportunity for a high-abundancy signal and off a greater amount of the ideal opportunity for a low-plentifulness signal.

**Pitch angle Controller:**

International Journal of Advances in Engineering and Management (IJAEM)
Volume 3, Issue 7 July 2021, pp: 881-895 www.ijaem.net ISSN: 2395-5252

Pitch angle control is the most common means for adjusting the aerodynamic torque of the wind turbine when wind speed is above rated speed and various controlling variables may be chosen, such as wind speed, generator speed and generator power.

**DC Link:**

A DC link is a connection which connects a rectifier and an inverter. These links are found in converter circuits and in VFD circuits. The AC supply of a specific frequency is converted into DC. This DC, in turn, is converted into AC voltage.

**Filter:**

Filters are a type of signal processing filter in the form of electrical circuits.These components can be in discrete packages or part of an integrated circuit. Electronic filters remove unwanted frequency components from the applied signal, enhance wanted ones, or both.

**Utility grid:**

**A utility grid** is normally a business electric force circulation framework that takes power from a generator (e.g., petroleum product kettle and generator, diesel generator, wind turbines, water turbine, and so on), sends it over a specific distance, at that point brings the power down to the shopper through a dissemination.

**MODELLING OF WIND TURBINE:**

The blades of a wind turbine rotate due to kinetic energy from the wind which is defined by the wind speed. An object with mass (m) which moves at velocity (v) has kinetic energy in the air givenby

$$E = \frac{1}{2} \times m \times V^2$$

The power contained in the moving blades assuming constant velocity is equal to the differential of this kinetic energy with respect to time as given

$$P_w = \frac{dE}{dt} = \frac{1}{2} \times m \times V^2 \quad (2)$$

where m represents the mass flow rate per second. When the air crosses the area "A" brushed by blades of the rotor, the power in air can be calculated with (Eq. 3).

$$P_w = \frac{1}{2} \times A \times V^3 \times \rho \quad (3)$$

ρ = the density of air.

Density of air can be conveyed as a component of the turbine's rise above sea level (H) as shown in Eq.4.

$\rho=\rho_0-1.194\times10^{-4}\times H$ (4)

where ρ0 = 1.225 kg/m3 which is the air density at sea level at temperature T = 298 K. The power extracted from wind is defined as,

$$P_{BLADE} = C_p(\lambda,\beta) \times P_\omega = C_p(\lambda,\beta) \times \frac{1}{2} \times v^3 \times A \times \rho \quad (5)$$

Cp = 0.593 (Betz law). The rotor power coefficient is a function of both the tip speed ratio "λ" and the blade pitch angle "β" (in degrees). The cutting edge pitch point is portrayed as the point between the sharp edge cross-region and the plane of revolution.It alludes to changing the attack angle to best suited angles to adjust the rotation speed of the blades hence adjusting generated power.

Tip speed ratio is defined in Eq.6,

$$\lambda = \frac{\omega_m \times R}{v}$$

$\omega_m$ is angular velocity of the rotor, R blade radius, and "wm*R" is the blade tip speed.

The rotor torque is therefore defined as,

$$T_w = \frac{P_{BLADE}}{\omega_m} = \frac{C_p(\lambda,\beta) \times \frac{1}{2} \times A \times \rho \times V^3}{\omega_m} \quad (7)$$

And, A, the area covered by the blade

$A = \pi \times R^2$

Substitute into Eq (6) and Eq (7) into Eq (8) .

$$T_w = \frac{P_{BLADE}}{\omega_m} = \frac{C_p(\lambda,\beta) \times \frac{1}{2} \times \pi \times R^2 \times \rho \times V^3}{\omega_m} \quad (8)$$

The power coefficient Cp can be expressed as shown in Eq.(8)

$$C_p(\lambda,\beta) = C_1 \times (C_2 \times \frac{1}{y} - C_3 \times \beta - C_4 \times \beta^x - C_5) \times e^{\frac{-C_6}{y}} \quad (9)$$

where gamma "y" is given as ,

$$\frac{1}{y} = \frac{1}{\lambda + 0.08\beta} - \frac{0.035}{1+\beta^2}$$

The Permanent magnet synchronous generator equation of motion as given is defined as:

International Journal of Advances in Engineering and Management (IJAEM)
Volume 3, Issue 7 July 2021, pp: 881-895 www.ijaem.net ISSN: 2395-5252

$$H_g \times \frac{dw_g}{dt} = T_e + \frac{T_m}{n} \quad (10)$$

where $T_e$ is Electromagnetic torque, $T_m$ is Mechanical torque, $T_w$ is wind torque.

Since the wind turbine shaft and generator are linked utilizing a gearbox, the shaft of the turbine is not viewed as stiff. Hence there will be movement in the shaft. The equation of motion of the drive train shaft is computed as

$$H_m \times \frac{dw_m}{dt} = T_w - T_m \quad (11)$$

Tm is given by

$$T_m = K \times \frac{\theta}{n} + D \times \frac{w_g - w_m}{n} \quad (12)$$

$$\frac{d\theta}{dt} = W_g - W_m \quad (13)$$

where, n is the gear ratio; θ is the angle between the turbine rotor and the generator rotor; Wm is the speed of the turbine; Wg is the speed of the generator; Hm is the turbine inertia constant; Hg is the generator inertia constant; K is drive train stiffness; and D is damping constant.

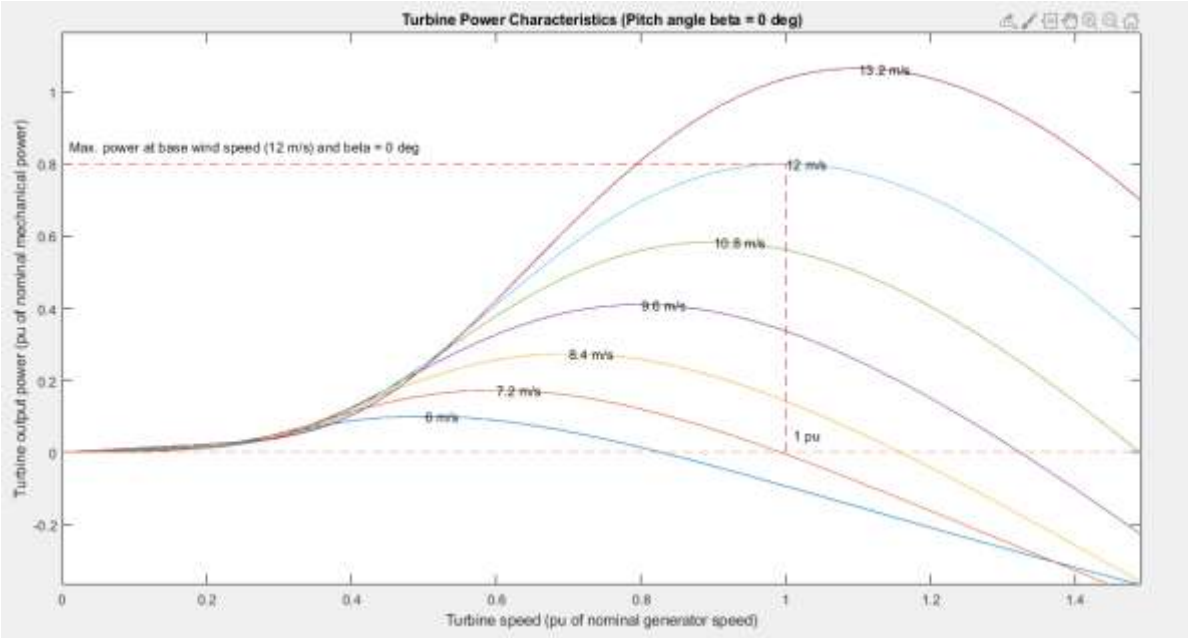


Simulation results:

This chapter deals with the results of the simulated circuits, models and characteristic analysis on components discussed in the previous chapters. It also includes design outputs and analysis outputs.

International Journal of Advances in Engineering and Management (IJAEM)
Volume 3, Issue 7 July 2021, pp: 881-895 www.ijaem.net ISSN: 2395-5252

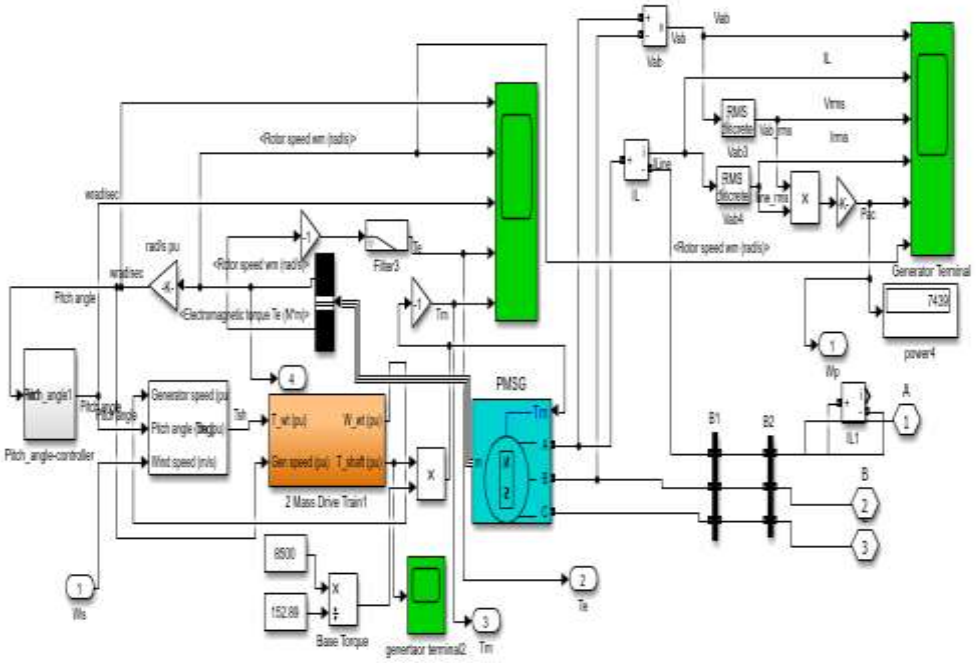


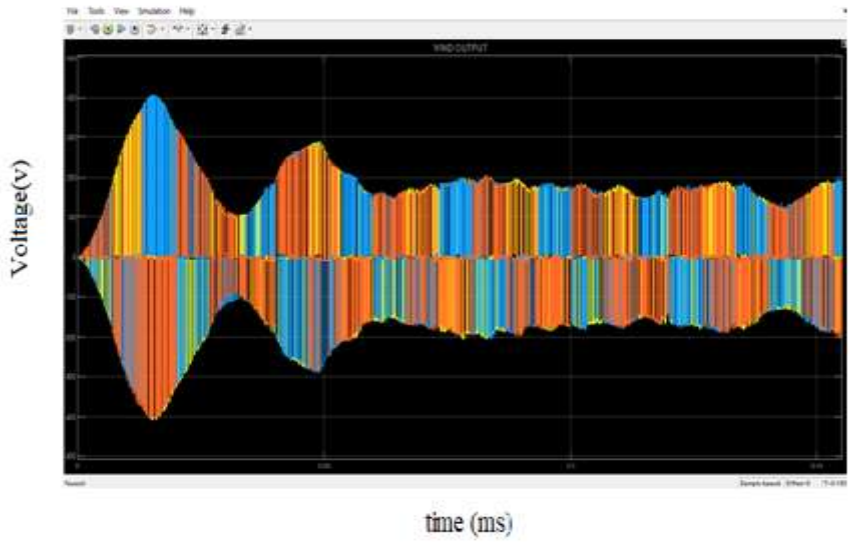

International Journal of Advances in Engineering and Management (IJAEM)
Volume 3, Issue 7 July 2021, pp: 881-895 www.ijaem.net ISSN: 2395-5252

**Three phase input of wind energy**

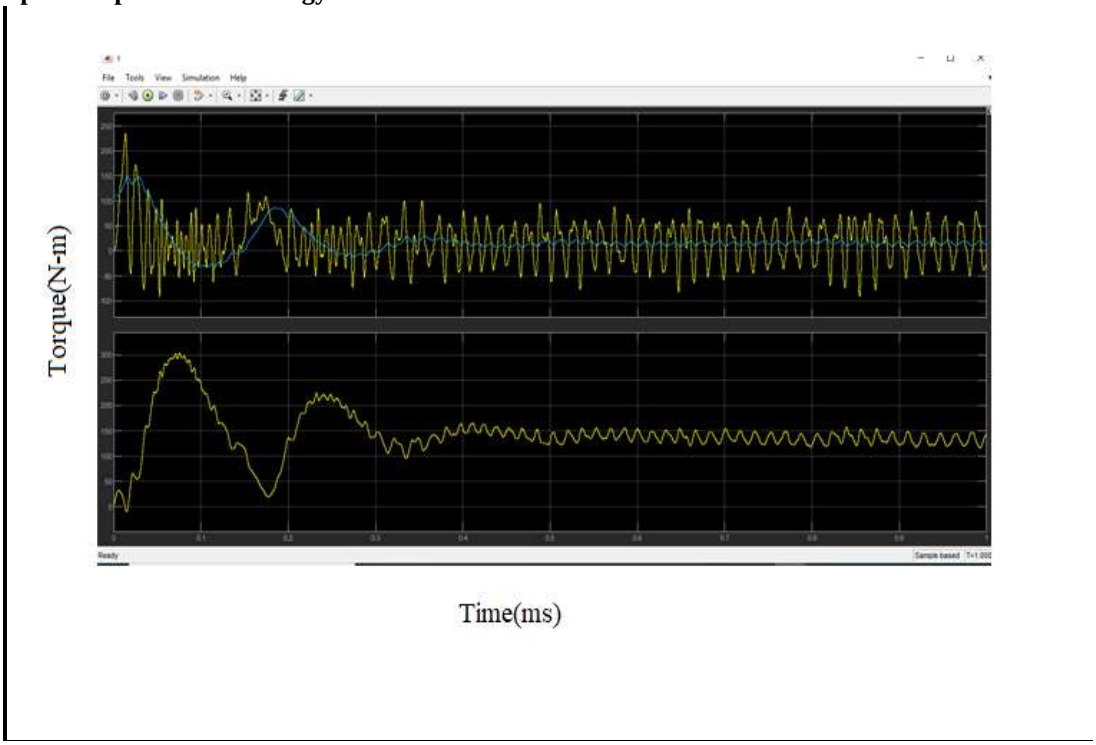


**Torque Of Wind Energy**

ffv

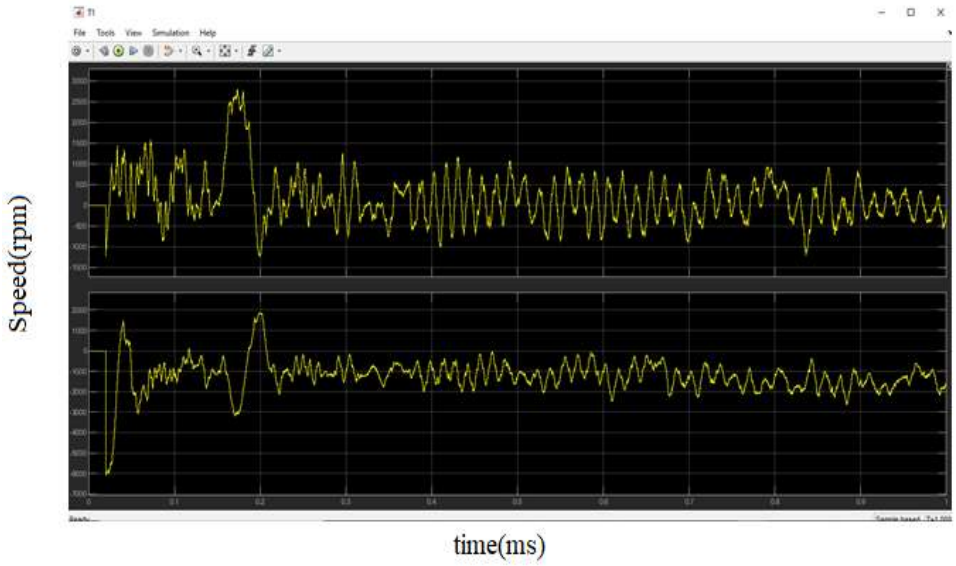


**Output waveform ofPMSG Wind generator**

International Journal of Advances in Engineering and Management (IJAEM)
Volume 3, Issue 7 July 2021, pp: 881-895 www.ijaem.net ISSN: 2395-5252

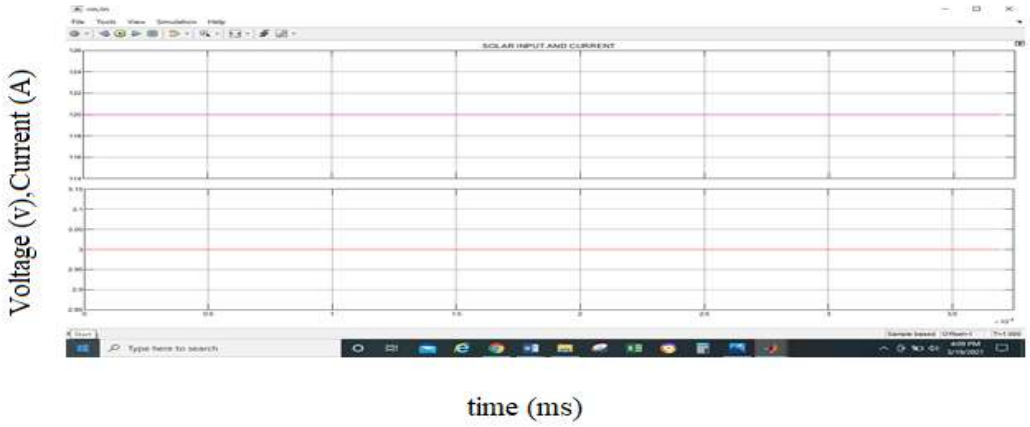


**Solar input voltage and current**

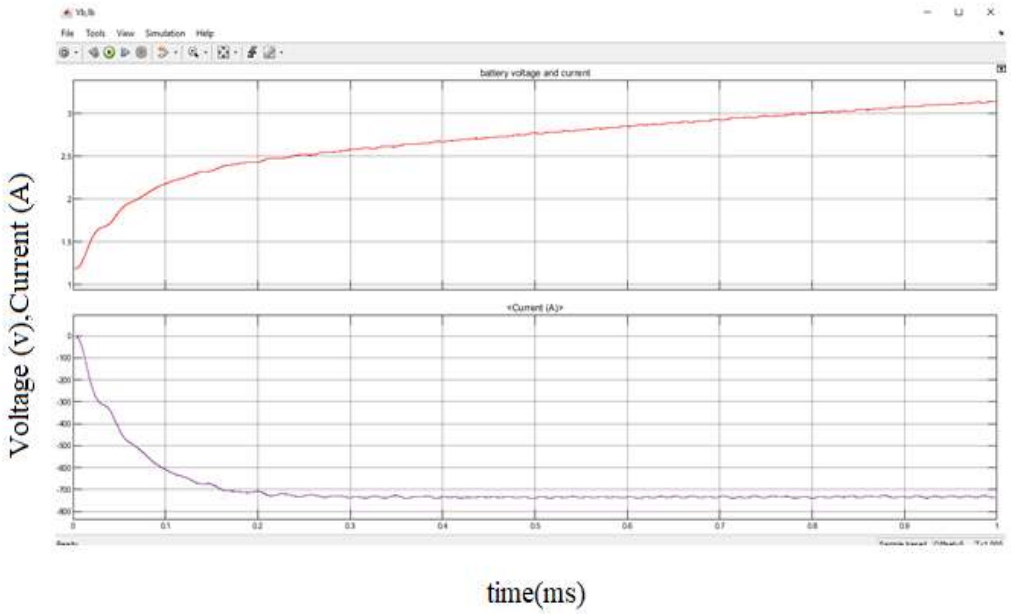


Battery output voltage and current

International Journal of Advances in Engineering and Management (IJAEM)
Volume 3, Issue 7 July 2021, pp: 881-895 www.ijaem.net ISSN: 2395-5252

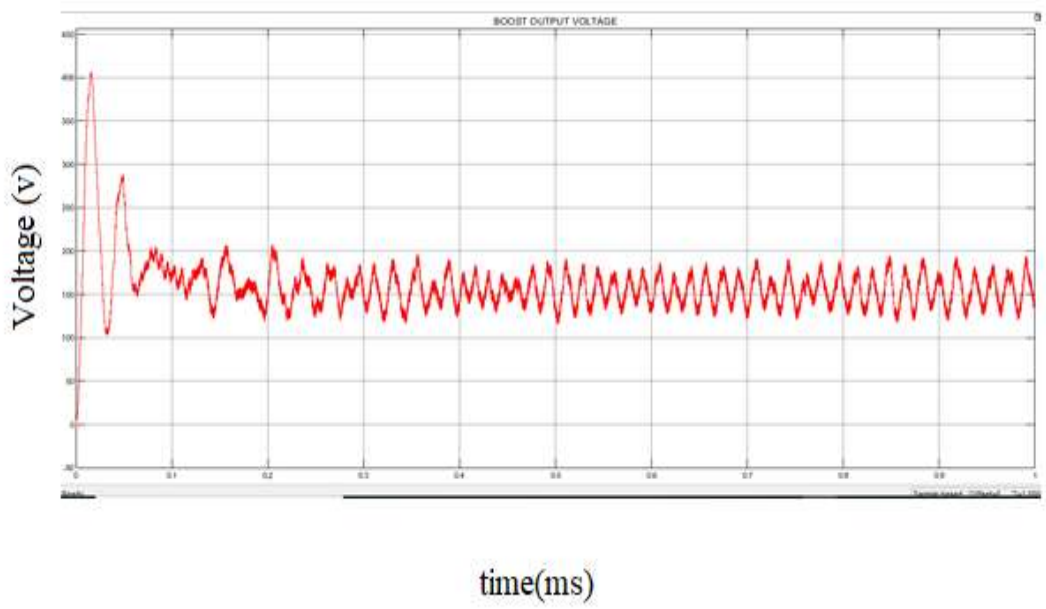


**Boost output voltage of solar energy**

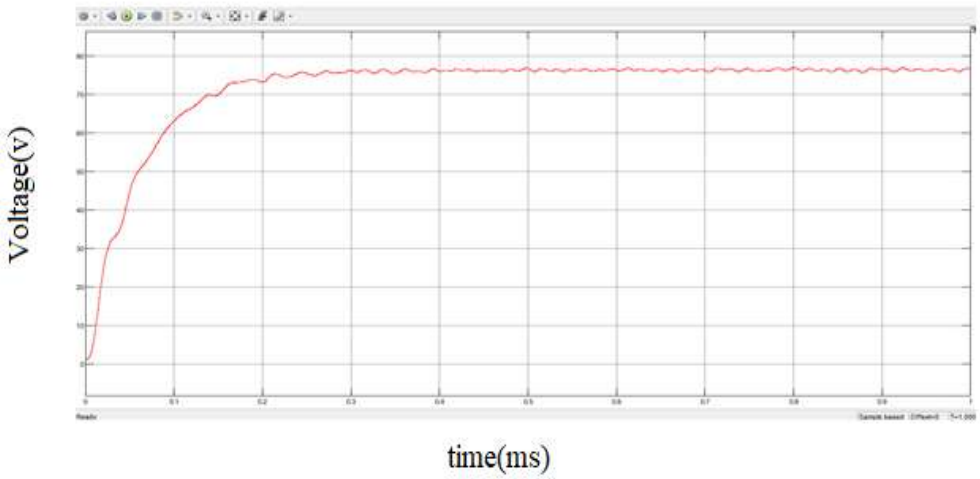


**Battery charging voltage**

## II. CONCLUSION

This paper has presented the wind-PV cogeneration systemsusing vector-controlled grid-connected BtB VSCs. The VSR at the wind generator-side is responsible for extracting the Maximum wind power following the wind speed variations. On the utility-grid side, the roles of the VSI are to extract the maximum PV power from the PV generator, achieve the balance between the input-output powers across the dc-link capacitor, and to maintain a unity PCC voltage under different modes of operation. A small-signal stability analysis has been conducted for the entire system. The proposed system has the following advantages; 1) the increased reliability and efficiency due to the combined wind and PV

generators. 2) The independent MPPT extraction as the VSR and VSI are solely responsible for extracting the wind and PV powers, respectively. 3) The regulation of the dc-link voltage under all operating conditions is maintained by the VSI and hence a better damped performance is yielded. 4) Simple system structure and controllers design. 5) fault-ride through can be achieved using existing protection schemes. A well-damped performance has been presented using time-domain simulations results under the Matlab/Simulink environment.

## REFERENCE

[1]. Renewable Energy Policy Network for the 21st Century, "Advancing theglobal renewable energy transition," REN21 Secretariat, Paris, France, 2017 [Available Online]

[2]. L. Nousiainen, J. Puukko, A. Maki, T. Messo, J. Huusari, J. Jokipii. J.Viinamaki, D. Lobera, S. Valkealahti, and T. Suntio, "Photovoltaic generator as an input source for power electronic converters," IEEETrans. Power Electron., vol. 28, no. 6, pp. 3028-3038, 2013.

[3]. Nicholas Strachan, and D.Jovcic,"Stability of a variable-speed permanent magnet wind generator with weak ac grids," IEEE Trans.Power Del., vol. 25, no. 4, pp.2279-2788, 2010.

[4]. P.Mitra, L. Zhang, and L. Harnefors, "Offshore wind integration to a weak grid by VSC-HVDC links using power-synchronization control – a case study," IEEE Trans. Power Del., vol. 29, no. 1, pp. 453-461, 2014.

[5]. Y. Wang, J. Meng, X. Zhang and L. Xu, "Control of PMSG-based wind turbines for system inertial response and power oscillation damping," IEEE Trans. Sustain. Energy, vol. 6, no. 2, pp. 565-574, 2015.

[6]. P. E. Bett and H. E. Thornton, "The climatological relationships betweenwind and solar energy in Britain," Renewable Energy, vo. 87, no. 1, pp. 96-110, 2016.

[7]. A. Merabet, K. Ahmed, H. Ibrahim, R. Beguenane, and A. Ghias, "Energymanagement and control system for laboratory scale microgrid based wind-pv-battery," IEEE Trans. Sustain. Energy, vol. 8, no. 1, pp. 145-154,2017.

[8]. K. Kant, C. Jain, and B. Singh, "A Hybrid diesel-wind-pv based energygeneration system with brushless generators," IEEE Trans. Ind. Inform., vol. 13, no. 4, pp. 1714-1722, 2017.

[9]. U. Kalla, B. Singh, S. Murthy, C. Jain and K. Kant, "Adaptive sliding mode control of standalone single-phase microgrid using hydro, wind and solar pv array based generation," IEEE Trans. Smart Grid, in press.

[10]. B. Mangu, S. Akshatha, D. Suryanarayana, and B. G. Fernandes, "GridconnectedPV-wind-battery-based multi-input transformer-coupled bidirectional dc-dc converter for household applications," IEEE Trans.Emerg. Sel. Topics Power Electron., vol. 4, no. 3, pp. 1086-1095, 2016.

[11]. P. Shanthi, G. Uma, and M. S. Keerthana, "Effective power transfer cheme for a grid connected hybrid wind/photovoltaic system," IETRenew. Power Gener., vol. 11, no. 7, pp. 1005-1017, 2017.

[12]. A. Radwan, Y. Mohamed, and E. El-Sadaany, "Assessment andperformance evaluation of DC-side interactions of voltage-source inverters interfacing renewable energy systems," Sustainable Energy,Grids and Networks Journal, vol. 1, pp. 28-44, 2015.

[13]. E. Troester, "New German grid codes for connecting PV systems to the medium voltage power grid," in Proc. 2nd Int. Workshop onConcentrating Photovoltaic Power Plant, pp. 1 – 4.

[14]. I. Abdelsalam, G. Adam, B. Williams, "Current source back-to-back converter for wind energy conversion systems," IET Renew. PowerGener., vol. 10, no. 10, pp. 1552-1561, 2016.

[15]. Mehrjerdi, H. (2020). Modeling, integration, and optimal selection of the turbine technology in the hybrid wind-photovoltaic renewable energy system design. Energy Conversion and Management, 205, 112350.

[16]. Li, S., Cai, Y. H., Schäfer, A. I., & Richards, B. S. (2019). Renewable energy powered membrane technology: A review of the reliability of photovoltaic-powered membrane system components for brackish water desalination. Applied Energy, 253, 113524.

[17]. Bingham, R. D., Agelin-Chaab, M., & Rosen, M. A. (2019). Whole building optimization of a residential home with PV and battery storage in The Bahamas. Renewable Energy, 132, 1088-1103.

[18]. Shin, H., &Geem, Z. W. (2019). Optimal design of a residential photovoltaic renewable system in South Korea. Applied

Sciences, 9(6), 1138.
[19]. Wong, C. Y., Wong, W. Y., Ramya, K., Khalid, M., Loh, K. S., Daud, W. R. W., ...&Kadhum, A. A. H. (2019). Additives in proton exchange membranes for low-and high-temperature fuel cell applications: a review. International Journal of Hydrogen Energy, 44(12), 6116-6135.
[20]. Young, S., Bruce, A., &MacGill, I. (2019). Potential impacts of residential PV and battery storage on Australia's electricity networks under different tariffs. Energy policy, 128, 616-627.
[21]. Atmaca, M., &Pektemir, I. Z. (2019). An investigation on the effect of the total efficiency of water and air used together as a working fluid in the photovoltaic thermal systems. Processes, 7(8), 516.
[22]. Hu, X., Ma, P., Wang, J., & Tan, G. (2019). A hybrid cascaded DC–DC boost converter with ripple reduction and large conversion ratio. IEEE Journal of Emerging and Selected Topics in Power Electronics, 8(1), 761-770.
[23]. Lo, K. Y., & Chen, Y. M. (2019). Design of a seamless grid-connected inverter for microgrid applications. IEEE Transactions on Smart Grid, 11(1), 194-202.
[24]. Xie, Z., Chen, Y., Wu, W., Xu, Y., Wang, H., Guo, J., &Luo, A. (2019). Modeling and control parameters design for grid-connected inverter system considering the effect of PLL and grid impedance. IEEE Access, 8, 40474-40484.
[25]. Al-Sarray, M. A. (2019). H2 Control for Improved Stability of Multi-area Electric Power System with High Levels of Inverter-Based Generation.
[26]. de Carvalho, R. S. (2019). Integrating Big Data Analytics and Cybersecurity for Power Distribution Networks with Distributed Energy Resources. Colorado School of Mines.